J. J. Trans. Phenomena, Vol. 10, pp. 103–112
Reprints available directly from the publisher
Photocopying permitted by license only

Micro Effects for Single Phase Pressure Drop In Microchannels

D. H. HAN[1†] AND M. A. KEDZIERSKI[2*]

[1] *Institute of Advanced Machinery, Design Korea University, 136-701 Seoul, Korea*
[2] *National Institute of Standards and Technology, Gaithersburg, MD 20899*

This paper investigates the significance of several "micro-effects" that have been proposed to influence pressure drop measurements in microchannels. Pressure drop measurements were made for liquid flow within tubular microchannels nominally ranging in diameters from 97 μm to 260 μm and Reynolds numbers from 30 to 3000. Fused silica tubes, polyetheretherketone tubes, and stainless steel tubes were examined. Distilled water, tap water, and deionized water were used to investigate the effect of the fluid's ionic composition on the pressure drop. The combination of differing tube surfaces and differing ionic composition was use to examine the influence of surface polarity. The effect of micro particles was investigated by testing filtered and unfiltered test fluids. Statistical examination of the measurements showed that most all of the friction factor measurements exhibited the same dependence on Reynolds number despite variation in tube length, tube material, tube diameter, fluid type, and filtering. In addition, the measurements agreed well with classical theory. This includes the fact that no early transition from laminar flow to turbulent flow was observed. Finally, it was shown that the present pressure drop measurements were not significantly affected by viscous dissipation.

Keywords: Pressure drop, single-phase, micro, microfluidics, microtechnology, micro devices

INTRODUCTION

Microtechnologies such as lab-on-a-chip systems and computer chip cooling rely heavily on the principles of microfluidics. As a result, the design of micro devices requires reliable microfluidic engineering tools. One key design element is the ability to predict single-phase pressure drop in microchannels for hydraulic diameters in the range of 10–100 μm. Not too long ago, the literature was approximately split

*Corresponding author: Mark.Kedzierski@NIST.gov
†Guest Researcher at the National Institute of Standards and Technology

between those that recommend the use of macro pressure drop equations for 20–300 mm channel diameters and those that did not. However, the tide has been turning in favor of the conclusion that, for the most part, conventional pressure drop theory can be used for microchannels. Because of this past confusion, the apparent cause of the difference between micro pressure drop measurements and macro prediction methods is not always clear (Kedzierski, 2003). In an effort to formalize the validity of using conventional pressure drop theory, this paper investigates the appropriateness of a few of the proposed "micro-effects" in a statistical approach as they apply to pressure drop measurements in microchannels.

One thing that is clear about the past state of the scientific literature on microchannel pressure drop measurements is that it is conflicting on when the classical (conventional) theory can be used to calculate the friction factor for microchannels. For example, Wu and Cheng (2003) found their pressure drop measurements to be in agreement with conventional theory for microchannels of trapezoidal cross-section with hydraulic diameters between 25.9 μm and 291.0 μm. Judy *et al.* (2002) also found good agreement with conventional theory for channel diameters between 15 μm and 150 μm for Reynolds number (Re) between 8 and 2300. Conversely, Pfund *et al.* (2000) showed that measured pressure drops in rectangular channels of depths between 128 μm and 521 μm differed from those predicted by the same classical theory. In contrast to this, the Mala and Li (1999) pressure gradient measurements for tube diameters larger than 150 μm showed agreement with conventional theory predictions as was shown by the Wu and Cheng (2003) measurements. However, for tube diameters less than 150 μm, the deviation from classical theory increased with increasing Re. For example, the Mala and Li (1999) pressure gradient measurements did not differ from conventional theory for a 130 μm diameter tube and a Reynolds number of 50. However, the conventional theory underpredicted the pressure gradient measurements for the same tube by approximately 70% for a Reynolds number of approximately 2100. Lastly, Brutin and Tadrist (2003) showed that depending on the fluid and the surface, agreement or significant disagreement between measurements and predictions can be realized for tube diameters greater than 150 μm (between 50 μm and 530 μm).

Many proposed reasons exist for the apparent difference between microchannel measurements and classical prediction theory. For example, Mala and Li (1999) suggested that the difference between measurement and predictions might be attributed to either surface roughness effects or early transition to turbulence. Xu *et al.* (2000) also observed an early transition to turbulent flow at Re $\approx$ 1500, which is significantly greater than the transition observed (Re 300 to 900) by Mala and Li (1999). Brutin and Tadrist (2003) minimize the influence of roughness by arguing that the effect of the polarity of the surface is significantly more important than surface roughness. Brutin and Tadrist (2003) propose that fluids with relatively large ionic concentrations like tap water can interact with the tube wall to create a "streaming [ionic] current" from the wall to the tube core. The streaming current is essentially a body force that acts as a local increase in viscosity causing an increase in the pressure drop. The streaming current was conjectured to be present for surfaces of both large and small polarizability (deactivated and activated fused silica). Brutin and Tadrist (2005) have since questioned their results. In addition, Baviere *et al.* (2005) did not find any micro effects as caused by differences in the electrical conductivity of water. Liu and Garimella (2004) suggest than no early transition to turbulent flow occurs for hydraulic diameters larger than approximately 200 μm. Sharp and Adrian (2004) also did not observe early transition for microtube diameters between 50 μm and 247 μm.

Besides roughness, early transition to turbulence, and surface polarity, two other popular micro effects are viscous dissipation and microscopic particles. Ghiaasiaan and Laker (2001) suggested that microscopic particles might be a major contributor to the inconsistency between classical theory and experimental measurements in microchannels. Xu *et al.* (2003) derived a criterion to predict the significance of viscous dissipation in microchannels.

As is evident from the above introduction, the established literature has neither decisively isolated the

TABLE 1
Fractional factorial experimental design

Tube acronym	Material	D_i [μm] ±95% conf. interval	L[mm] ± 5 μm	Test Fluid	0.5 μm filter used
1DL10	FS	97.86 ± 2.02	99.73	Distilled water	yes
1DL5	FS	97.20 ± 2.04	50.14	Distilled water	yes
2DL10	PEEK	146.84 ± 0.33	101.91	Distilled water	yes
2DL5	PEEK	144.85 ± 0.41	50.97	Distilled water	yes
3DL10	SS	134.49 ± 0.23	100.01	Distilled water	yes
3DL5	SS	130.67 ± 0.81	50.04	Distilled water	yes
4DL15	PEEK	257.53 ± 1.06	152.02	Distilled water	yes
4DL10	PEEK	260.39 ± 0.71	103.53	Distilled water	yes
2IL10	PEEK	146.84 ± 0.33	101.91	Deionized water	yes
2TL10	PEEK	146.84 ± 0.33	101.91	Tap water	yes
2TNFL10	PEEK	146.84 ± 0.33	101.91	Tap water	no
3IL10	SS	134.49 ± 0.23	100.01	Deionized water	yes
3TL10	SS	134.49 ± 0.23	100.01	Tap water	yes

salient micro effects nor determined when and where classical theory can be applied to the prediction of pressure drops in microchannels. Consequently, the present study contributes to the microchannel pressure drop data with the aim of examining some of the key micro effects. Table 1 shows the fractional factorial experimental design by listing the circular tubes and the test conditions that were used to investigate the effects of tube length, tube material, tube diameter, fluid type, and microscopic particles (filtering). The pressure drop was measured for 13 different test sections. Three different tube materials were used to investigate the effect of tube surface on the pressure drop: "activated" fused silica (FS), polyetheretherketone (PEEK), and stainless steel (SS). In addition, the effect of the polarity of the surface was examined by testing fluids of differing ionic compositions: distilled water, deionized water, and tap water. The influence of microscopic particles was also studied by making measurements with and without a 0.5 μm filter. The effect of entry length was examined with three different nominal tube lengths of 50 mm, 100 mm, and 150 mm. A range of tube diameters was chosen between nominally 97 μm and 260 μm to determine if a transition from "micro" to classical theory exists for Reynolds numbers between roughly 30 and 3000. To more easily grasp the investigated range of parameters, Table 2 summarizes the experimental conditions of this study.

APPARATUS

Figure 1 shows a schematic of the test loop that was used to measure the pressure drop and the flow rate for the various circular cross-sectioned microchannels shown in Fig. 2. A high-pressure (2 MPa maximum) gear pump drew the test fluid from the bottom of a 120 L reservoir and supplied the test section with liquid flow. The reservoir was partially filled with 40 L to 50 L of test fluid. A 20 μm pore filter was placed between the exit of the reservoir and the suction of the pump. The flow rate delivered to the test section was regulated with a combination of a coarse valve in the pump bypass and a linear metering valve prior to the test section. A cold-water bath and a heat exchanger were used to remove the heat added to the loop by the pump and maintain the loop at a temperature equal to the ambient room temperature. Maintaining the loop temperature at ambient and insulating the test section encouraged an adiabatic test section. An expansion tank prior to the metering valve was used to dampen flow fluctuations that may have been introduced by the pump.

TABLE 2
Summarized experimental parameter ranges

Parameter	Minimum	Maximum	Average $U(\%)$
Re	26	2977	2.13
f	0.04	2.75	6.42
Po	15	33	5.96
$\dot{m}$ [kg/s]	1.75×10^{-6}	5.21×10^{-4}	1.17
L [mm]	50.04	152.02	3.56
D_i [μm]	97.20	260.39	2.99
ΔP_T [N/m^2]	22301	971674	3.22

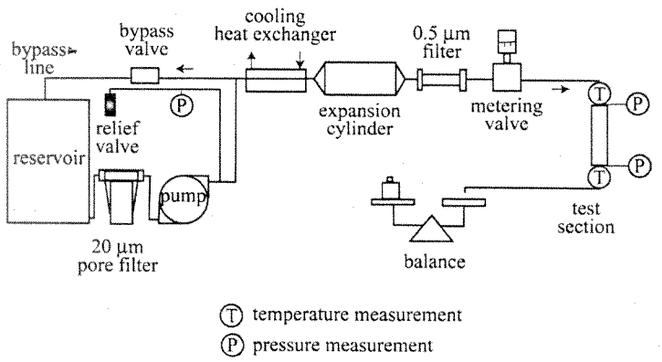

FIGURE 1
Schematic of test apparatus.

MEASUREMENTS AND UNCERTAINTIES

The standard uncertainty (u_i) is the positive square root of the estimated variance u_i^2. The individual standard uncertainties are combined to obtain the expanded uncertainty (U), which is calculated from the law of propagation of uncertainty with a coverage factor. All measurement uncertainties are reported at the 95% confidence level except where specified otherwise.

Temperature and Pressure

Figure 3 schematically shows the design of the temperature and pressure measurement ports for the test section. Two 0.79 mm outside diameter T-type thermocouples were used to measure the inlet and outlet temperature of the test section. The thermocouples were calibrated to an expanded uncertainty less than ±0.06 K. Thermopiles were not used due to the difficulty of installing the required many elements in micro diameter tubes. Two separate pressure transducers were used to measure the pressure drop across the inlet and outlet of the test section. Use of a differential pressure transducer would have reduced the measurement uncertainty by at least 40%; however, because of the relatively large pressure drops for microchannels the uncertainty of the measurement remained at acceptable levels. The entrance and the exit pressure transducers were calibrated to an expanded uncertainty of ±0.7 kPa and ±0.4 kPa, respectively. The resulting maximum expanded uncertainty for differential pressure was 0.6% of the measurement. The pressure drop in the 4.8 mm length of 1.25 mm internal diameter tube leading to the test section (see Fig. 3) was calculated

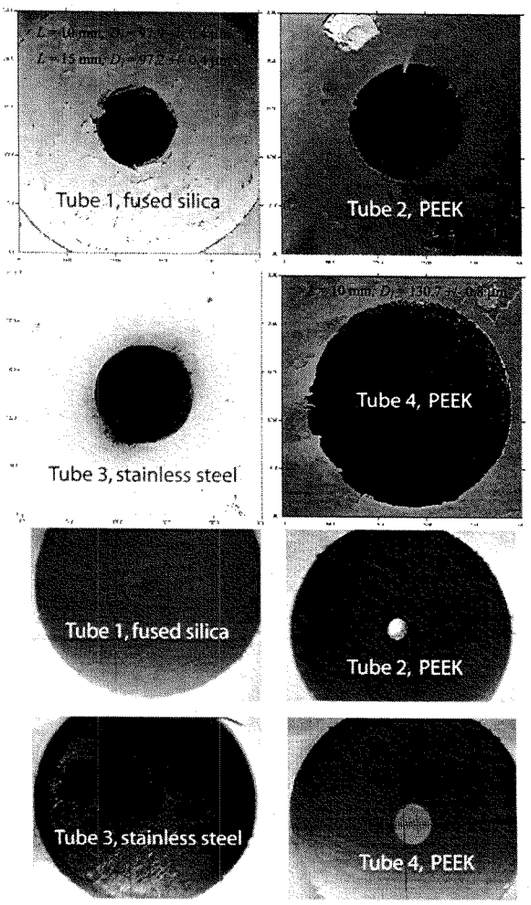

FIGURE 2
Cross sections of test microchannels.

from classical theory and subtracted from the total pressure drop measurement. The correction for the inlet and outlet 4.8 mm lengths from the test section to the pressure ports was between 0.02% and 0.002% of the total pressure drop.

Reynolds Number

Figure 1 schematically shows the 200 g equal-arm balance that was used to measure the flow rate exiting the test section via a time-weight methodology. A "standard" weight of 5 g, 10 g, 15 g, or 20 g was placed on the left pan while a vessel for capturing the test fluid

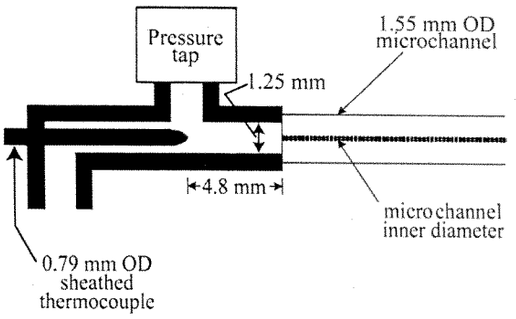

FIGURE 3
Experimental design for temperature and pressure measurement for inlet and exit of test section.

was placed on the right pan. The equal-arm balance was chosen because the standard weights could be readily placed and removed on/from the pan and the motion of the arm could be easily observed. A steady rate of flow into the collection pan was established while having a sufficient weight on the left pan to keep the collection pan fully elevated during this period. The fill time was initiated when the collection pan began to descend. At this point an additional mass was added to the left pan to fully elevate it again. The recorded time was stopped when the collection pan began to descend again. This completed the test run for a single data point and the test fluid was poured back into the reservoir. The expanded uncertainty of the mass flow rate ($\dot{m}$) using the time-weight method was estimated to be between $\pm 1\%$ and $\pm 4.7\%$ of the measurement. The mass flow rate was used to calculate the Reynolds number of the flow from:

$$\mathrm{Re} = \frac{4\dot{m}}{\bar{\mu}\pi D_i} \tag{1}$$

where D_i is the internal diameter of the round tube, and $\bar{\mu}$ is the dynamic viscosity of the test fluid evaluated at its average temperature in the test section. The diameter of each tube was measured at both ends with a microscope. In addition, the diameters of the PEEK tubes (tubes 2 and 4) were destructively measured at points along the length. Repeated measurements were averaged for each tube to obtain the mean diameter and the associated expanded uncertainty and are given in Table 1. The expanded uncertainty of D_i varied between approximately $\pm 0.2\,\mu$m and $\pm 2.0\,\mu$m

TABLE 3
Estimated uncertainties

Tube acronym	$U_{\dot{m}}$ [%]	U_{Re}[%]	U_f [%]
1DL10	4.696	6.199	16.884
1DL5	4.654	6.213	14.122
2DL10	0.945	1.086	5.513
2DL5	0.944	1.101	9.080
3DL10	4.704	4.717	9.452
3DL5	4.634	4.791	9.955
4DL15	0.935	1.237	8.148
4DL10	0.939	1.089	12.225
2IL10	2.618	3.128	7.356
2TL10	1.667	2.390	5.912
2TNFL10	1.667	2.388	5.837
3IL10	4.690	5.758	12.676
3TL10	2.636	4.255	10.068

depending on the microchannel test section. Considering the uncertainties in the measured diameter and the mass flow rate, the expanded uncertainty of Re was between ±1% and ±6.2% of the measurement as shown in Table 3.

The variation in the uncertainties of the mass flow rate and Re is due largely to the variation in the uncertainty of the tube diameter measurement. For the most part, the larger Re and $\dot{m}$ uncertainties correspond to the larger uncertainties in D_i.

Friction Factor and Poiseuille Number

The Fanning friction factor (f) was obtained by separating the fully developed frictional pressure drop (ΔP_f) from the total measured pressure drop (ΔP_T) and its minor components as:

$$\Delta P_f = \Delta P_T - \Delta P_e - \Delta P_{df} - \Delta P_m \qquad (2)$$

where ΔP_e is the entrance and exit pressure drop, ΔP_{df} is the pressure drop in the hydrodynamic developing flow region, and ΔP_m is the momentum pressure drop. Figure 4 shows the importance of the non-frictional pressure drops relative to the total pressure drop measurement.

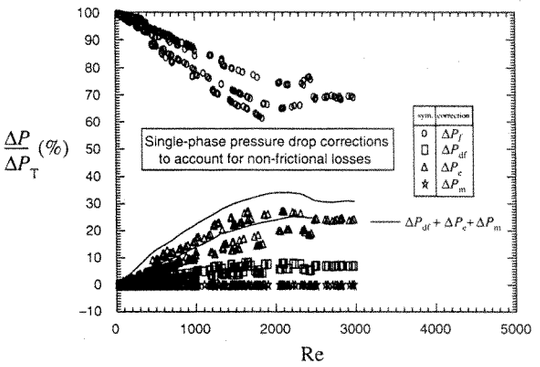

FIGURE 4
Single-phase pressure drop corrections to account for non-frictional losses.

The momentum pressure drop results from the difference between the fluid density at the entrance (ρ_i) and the exit (ρ_o) of the test section that is induced by viscous heating:

$$\Delta P_m = \frac{G^2}{\rho_i}\left(\frac{\rho_i}{\rho_o} - 1\right) \qquad (3)$$

where G is the total mass velocity within the tube. The maximum measured temperature difference between the inlet and the outlet of the test section did not exceed 0.1 K. As a result, the momentum pressure drop shown in Fig. 4 was negligibly small being approximately 1×10^{-6}% of the total pressure drop.

The entrance and exit pressure drop was calculated with the loss coefficients (K) and the mean fluid velocity (u_m) defined as:

$$\Delta P_e = K\frac{\bar{\rho}u_m^2}{2} \qquad (4)$$

where $\bar{\rho}$ is the average density of the fluid in the test section and the mean velocity was calculated from the measured mass flow rate. Because of the small contraction and expansion ratios for the test section, the loss coefficients for the sudden contraction at the entrance and that for the sudden expansion at the exit were taken as approximately $K = 0.5$ and $K = 0.95$, respectively (Fox and McDonald, 1992). As shown in Fig. 4, the sum of the entrance and pressure losses remained less than 20% of the total pressure drop for all of the measurements.

The developing flow pressure drop was calculated from a correlation given by Shah and London (1978):

$$\Delta P_{df} = \frac{1}{2}\bar{\rho}u_m^2\left(13.74\sqrt{L_{df}^+} + \frac{1.25 + 64L_{df}^+ - 13.74\sqrt{L_{df}^+}}{1 + 0.00021(L_{df}^+)^{-2}}\right) \quad (5)$$

The L_{df}^+ is the dimensionless hydrodynamic developing flow entrance length:

$$L_{df}^+ = \frac{L_{df}/D_i}{\mathrm{Re}} \quad (6)$$

and L_{df} is the dimensional hydrodynamic developing flow entrance length.

Shah and London (1978) proposed the following to describe L_{df}^+ for Re > 400:

$$L_{df}^+ = 0.0565 \quad (7)$$

For Re < 400, Chen (1973) proposed following equation for L_{df}^+:

$$L_{df}^+ = 0.056 + \frac{0.60}{\mathrm{Re}(1 + 0.035\mathrm{Re})} \quad (8)$$

Figure 4 shows that the pressure drop due to developing flow was less than 10% of the total pressure drop. In addition, the solid lines in Fig. 4, which represent the sum of the non-frictional pressure drops, are shown to be less than 35% of the total pressure drop for all Re. Lee *et al.* (2005) showed that good agreement of their microchannel heat transfer measurements with numerical predictions were, in large part, due to carefully accounting for the entrance and boundary conditions of the experiment. By analogy, careful consideration of pressure drop entrance effects are required to correctly reduce microchannel pressure drop data.

The Fanning friction factor (f) was calculated from the frictional pressure drop and the length of the test section associated with fully developed frictional flow (L_f) as:

$$f = \frac{D_i \Delta P_f}{2\bar{\rho}u_m^2 L_f} = \frac{\pi^2 D_i^5 \bar{\rho}\Delta P_f}{32\dot{m}^2 L_f} \quad (9)$$

Table 3 shows that the expanded uncertainty of the Fanning friction factor was between approximately ±5.5% and ±17% of the measurement.

The Poiseuille number (Po) can be calculated from the measured frictional pressure drop, the average fluid properties, and the measured mass flow rate as:

$$\mathrm{Po} = f\mathrm{Re} = \frac{\pi D_i^4 \bar{\rho}\Delta P_f}{8\bar{\mu}L_f\dot{m}} \quad (10)$$

As can be seen with the above equations, the Poiseuille number and the friction factor are dependent on the diameter to the fifth and the forth power, respectively. As a result, the relative uncertainty of the diameter measurement dominates the overall uncertainties of Po and f.

EXPERIMENTAL RESULTS

Figure 5 plots all the measured Fanning friction factors of this study for Reynolds numbers between 30 and 3000. The figure legend shows the symbols and the acronyms that were used to represent each data set. The acronyms for the data sets are defined in Table 1. Regression of the friction factor versus Re^{-1} through the origin (for Re < 2000) was done while including an additional variable that identified a specific data set. The statistical significance of the "set variable" in the

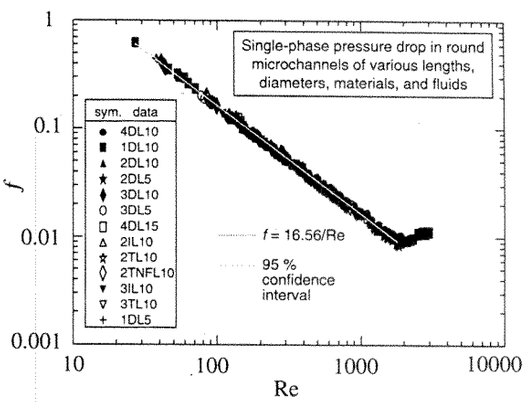

FIGURE 5
Single-phase pressure drop characteristic of round microchannels (see Table 1).

regression was used as the criteria for determining if a particular data set belonged to the larger set. In this way, the method identified any statistically significant deviation from the core data set, which could be used to identify a specific micro effect. The results of the methodology showed that all of the data sets except data sets 3DL5, 3IL10, and 3TL10 statistically belonged to a single combined "core" data set. The excluded data sets were all but one of the data sets for the stainless steel tubes. The mean Poiseuille number for the 3DL5, 3IL10, and 3TL10 data sets was 6.1%, 5.7% and 7.3% less than that obtained for the core data set, respectively. Similarly, the mean Poiseuille number for the 3DL5, 3IL10, and 3TL10 data sets was 2.8%, 2.4%, and 4.0% less than that given by classical theory (Kays and Crawford, 1980), respectively.

Figure 5 shows that the transition to turbulence occurs at approximately Re = 2000. Regression of f = Po/Re for the core data set for Re less than 2000 gave a mean Poiseuille number of 16.56 ± 0.06, which is 3.5% greater than the conventional theory (Po = 16). A solid gray line against the data symbols represents the regression. The average 95% confidence intervals on the mean Fanning friction factor is approximately ±0.0004, which is, on average, approximately 0.6% of the friction factor.

Choice of Regression Model

The Poiseuille number could have been determined by either one of two regressions. As outlined above, the Po in this study was determined from a regression of the friction factor versus Re^{-1} through the origin. This decision was based on following the Gauss-Markov theorem (Neter *et al.*, 1990) that states that the least square estimates have the smallest regression variances. The small variances is attributed to the use of a weighted average of the f's for the f = Po/Re regression. Conversely, the $f \cdot Re$ = Po regression does not have the advantage of weighted f's and consequently does not provide the best fit of the data. Even though it would be tempting to use the $f \cdot Re$ = Po fit because of its directness with respect to Po, it does not faithfully represent the measurements as well as the f = Po/Re fit. This point is illustrated by the results of $f \cdot Re$ = Po regression which gave Po = 16.70 and a correspondingly larger uncertainty of ±0.09.

DISCUSSION

Statistical examination of the measurements showed that most all of the friction factor measurements exhibited the same dependence on Re despite variation in tube length, tube material, tube diameter, fluid type, and filtering. Even those data that were deemed to not belong to the core data set were outliers by only a few percent (6.1% to 7.3%). Consequently, if the existence of outlier data sets indicates that a micro effect exists, the effect is relatively insignificant in this study.

Given that the only commonality for the outliers is that they were all for nominally 130 μm diameter stainless steel tubes, while having differing ionic concentrations and different tube lengths, it must be assumed that the effect is one for which the experiment was not designed to test. Lacking any plausible reason for the effect, the outliers were likely caused by some unknown experimental error and/or bias. However, it is unlikely that a burr at the tube entrance or exit caused a measurement error because the data set 3DL10, which is part of the core data set, used the same tube that was used for the outlying 3IL10, and 3TL10 data sets. It is also unlikely that ionic composition differences influenced the outliers because both the core data set and the outlier data sets contained all three different ionic compositions (distilled water, deionized water, and tap water). The fact that all three outlier data sets used SS tubes may also be disregarded because one of the SS tubes was part of the core data set.

The test matrix shown in Table 1 is by no means a full factorial design experiment. Nevertheless, some key observations, while ignoring possible coupling that may have been exposed by a full factorial design, can be made regarding the influence of micro effects on the measurements of this study. For example, the core data set contained measurement for all of the tube lengths of this study indicating that tube length was not a micro effect and that the conventional entry length pressure drop calculations were done properly. The core data set also contained all the tube diameters examined

in the study suggesting that no micro effects due to tube diameter were present for diameters between 97 μm and 260μm. The core data set also contained 0.5 μm filtered and unfiltered measurements showing that microscopic particles did not affect the measurements. In addition, core data set contained all three different tube materials (FS, PEEK, and SS) and all three testing fluids of differing ionic compositions suggesting that neither tube roughness nor surface polarity influenced the pressure drop measurements. Finally, the observed transition Re number of 2000 did not differ greatly from that observed for macro tubes.

In general, roughness has little effect on the pressure drop for laminar flow. This is also apparently true for microchannel flow. For example, the numerical analysis of Croce and D'Agaro (2004) showed that the Poiseuille number for microtubes (for Re $<$ 1800) was increased by a mere 6% for a roughness ratios as large as 0.013. It took a roughness ratio of 0.053 to produce a laminar Poiseuille number approximately 41% larger than that value traditionally given (Po = 16). The nominal RMS roughness* values for the inside of the SS and FS tubes for the present study were 63 nm and 5 nm, respectively (Zahn, 2005), and the RMS roughness of the inside of the PEEK tube was 5 nm (Bartolo *et al.*, 2005). The corresponding roughness ratio for the SS, the FS, and the PEEK tubes were approximately 0.0005, 0.00005, and 0.00003, respectively. Given the relatively small roughness ratios, it is not surprising that surface roughness does not appear to affect the Poiseuille number for the present data.

Xu *et al.* (2003) emphasized the effect of viscous dissipation in microchannels that result in temperature induced changes in fluid viscosity resulting in changing viscous shear forces. The radial pressure distribution and the Re are altered as a result of the changing viscous shear forces in the flow direction. The dimensionless analysis criterion of Xu *et al.* (2003) indicated that the measurements of the present study are in the region of "no viscous dissipation effects." In addition, the maximum viscous dissipation induced inlet-outlet temperature difference for a laminar, incompressible fluid was calculated using an expression given by Suryanarayana (1995) and was found to not exceed 0.15 K. The corresponding temperature rise would be responsible for a 0.3% change in the viscosity of water at room temperature. Consequently, it is believed that this confirms the Xu *et al.* (2003) analysis that the present data are not significantly affected by viscous dissipation.

*Vorburger and Raja (1990) provide clear definitions of roughness parameters.

CONCLUSIONS

In general, the present liquid pressure drop measurements exhibited no significant deviation from classical theory for tube diameters between 97 μm and 260 μm and Reynolds numbers from 30 to 3000. In addition, the transition Re number was observed to be approximately 2000, which does not significantly differ from that taught by traditional theory. Statistical examination of the measurements showed that most all of the friction factor measurements exhibited the same dependence on Re despite variation in tube length, tube material, tube diameter, fluid type, and filtering. In other words, microscopic particles where not shown to affect the measurements. Also, the testing of three different tube materials and three different ionic concentrations of water suggested that neither tube roughness nor surface polarity influenced the pressure drop measurements. Given the relatively small roughness ratios, it is not surprising that surface roughness does not appear to affect the Poiseuille number for the present data. Finally, it was shown that the present pressure drop measurements were not significantly affected by viscous dissipation.

ACKNOWLEDGEMENTS

The National Institute of Standards and Technology and the Post-doctoral Fellowship Program of Korea Science and Engineering Foundation (KOSEF) jointly funded this work. Thanks go to the following people for their constructive criticism of the first draft of the manuscript: Mr. D. Yashar, Dr. P. Domanski, and Dr. D. Didion (retired) of NIST and Dr. J. Kim of the University of Maryland. Furthermore, the author extends

appreciation to Dr. W. Guthrie and Mr. A. Heckert of the NIST Statistical Engineering Division for their consultations on the uncertainty analysis.

NOMENCLATURE

D_i	inner diameter, m
f	dimensionless Fanning friction factor
G	mass flux, kg/m^{2}s
K	loss coefficient
L	test section length, m
L_f	test section length associated with fully developed frictional flow ($L - L_{df}$), m
L_{df}^+	dimensionless hydrodynamic developing entrance length
L_{df}	hydrodynamic developing entrance length, m
$\dot{m}$	mass flow rate, kg/s
Po	dimensionless Poiseuille number (eq. 10)
Re	dimensionless Reynolds number
u_m	mean fluid velocity, m/s

Greek Symbols

ΔP	pressure drop, N/m^2
ρ	fluid density, kg/m^3
$\bar{\rho}$	average fluid density, kg/m^3
$\bar{\mu}$	average liquid dynamic viscosity, kg/m·s

Subscripts

df	developing flow
e	entrance and exit
f	frictional
i	inlet
m	momentum
o	outlet
T	total

REFERENCES

Baviere, R., Ayela, F., Le Person, S., and Favre-Mrinet, M., 2005, "Experimental Characterization of Water Flow Through Smooth Rectangular Microchannels," *Physics of Fluids*, **17**, 098105.

Brutin, D., Tadrist, L., 2005, "Comments on 'A Study of Laminar Flow of Polar Liquids Through Circular Microtubes'," *Physics of Fluids*, **17**, 019101.

Brutin, D., Tadrist, L., 2003, "Experimental Friction Factor of a Liquid Flow In Microtubes," *Physics of Fluids*, **15**(3), 653–661.

Chen, R. Y., 1973, "Flow in the Entrance Region at Low Reynolds Numbers," *J. Fluids Eng.*, **95**, 153–158.

Croce, G., and D'Agaro, P., 2004, "Numerical Analysis of Roughness Effect on Microtube Heat Transfer," *J. Superlattices and Microstructures*, **35**, 601–616.

De Bartolo, L., Gugliuzza, A., Morelli, S., Cirillo, B., Gordano, A., Drioli, E., 2005, "Physico-Chemical Properties and Performance of Novel PEEK-WV Membranes Contacting Human Plasma and Proteins," *Materials Science Forum*, **480–481**, 257–268.

Fox, R. W., and McDonald A. T., 1992, *Introduction to Fluid Mechanics*, 4th ed., Wiley, New York, p. 355.

Ghiaasiaan, S. M., Laker, T. S., 2001, "Turbulent Forced Convection in Microtubes," *International Journal of Heat and Mass Transfer*, **44**, 2777–2782.

Judy, J., Maynes, D., and Webb, B.W., 2002, "Characterization of Frictional Pressure Drop for Liquid Flows Through Microchannels," *IJHMT*, **45**, 3477–3489.

Lee, P., Garimella, S. V., and Liu, D., 2005, "Investigation of Heat Transfer in Rectangular Microchannels," *IJHMT*, **48**, 1688–1704.

Liu, D. and Garimella, S. V., 2004, "Investigation Of Liquid Flow in Microchannels," *J. Thermophysics and Heat Transfer*, **18**(1), 65–72.

Kays, W. M. and Crawford, M. E., 1980, *Convective Heat and Mass Transfer*, McGraw Hill Book Co., 2nd ed., New York, p. 62.

Kedzierski, M. A., 2003, "Micro Channel Heat Transfer, Pressure Drop And Macro Prediction Methods," Keynote for 2nd International Conference on Heat Transfer, Fluid Mechanics and Thermodynamics, June 23–26, Victoria Falls, Zambia.

Mala, G. M., Li, D., 1999, "Flow Characteristics of Water in Microtubes," *International Journal of Heat and Fluid Flow*, **20**, 142–148.

Neter, J., Wasserman, W., and Kutner, M. H., 1990, *Applied Linear Statistical Models*, 3rd ed., Richard D. Irwin, Inc., Burr Ridge, p. 43.

Pfund, D., Rector, D., Shekarriz, A., Popescu, A., Welty, J., 2000, "Pressure Drop Measurements in a Microchannel," *AIChE Journal*, **46**(8), 1496–1507.

Shah, R. K., and London, A. L., 1978, "Laminar Flow Forced Convection in Ducts," *Supplement 1 to Advances in Heat Transfer*, eds. Irvine, T. F. and Hartnett, J. P., Academic Press, New York.

Sharp, K. V., and Adrian, R. J., 2004, "Transition from Laminar to Turbulent Flow in Liquid Filled Microtubes," *Experiments in Fluids*, **36**, 741–747.

Suryanarayana, N. V., 1995, *Engineering Heat Transfer*, West Pub. Co., St. Paul.,

Vorburger, T. V., and Raja, J., 1990, "Surface Finish Metrology Tutorial," NISTIR 89-4088, U.S. Department of Commerce, Washington.

Wu, H. Y. and Cheng, P., 2003, "Friction Factors in Smooth Trapezoidal Silicon Microchannels with Different Aspect Ratios," *International Journal of Heat and Mass Transfer*, **46**, 2519–2525.

Xu, B., Ooi, K. T., Wong, N. T. and Choi, W. K., 2000, "Experimental Investigation of Flow Friction for Liquid Flow in Microchannels," *Int. Comm. Heat mass Transfer*, **27**, 1165–76.

Xu, B., Ooi, K. T., Mavriplis C. and Zaghloul, M. E., 2003, "Evaluation of Viscous Dissipation in Liquid Flow in Microchannels," *J. Micromech. Microeng*, **13**, 53–7.

Zahn, C., 2005, Private communications.